Available online at www.sciencedirect.com
ScienceDirect
Fuel xxx (2007) xxx–xxx
FUEL
www.fuelfirst.com

Model development and validation: Co-combustion of residual char, gases and volatile fuels in the fast fluidized combustion chamber of a dual fluidized bed biomass gasifier

Priyanka Kaushal *, Tobias Pröll, Hermann Hofbauer

Vienna University of Technology, Institute of Chemical Engineering, Getreidemarkt 9/166, A-1060, Vienna, Austria

Received 20 November 2006; received in revised form 14 March 2007; accepted 20 March 2007

Abstract

A one-dimensional steady state model has been developed for the combustion reactor of a dual fluidized bed biomass steam gasification system. The combustion reactor is operated as fast fluidized bed (riser) with staged air introduction (bottom, primary and secondary air). The main fuel i.e., residual biomass char (from the gasifier), is introduced together with the circulating bed material at the bottom of the riser. The riser is divided into two zones: bottom zone (modelled according to modified two phase theory) and upper zone (modelled with core-annulus approach). The model consists of sub-model for bed hydrodynamic, conversion and conservation. Biomass char is assumed to be a homogeneous matrix of C, H and O and is modelled as partially volatile fuel. The exit gas composition and the temperature profile predicted by the model are in good agreement with the measured value.

Keywords: Model; Fluidized bed; Char combustion

1. Introduction

Currently, biomass fuel provides 15% of world's primary energy and this fulfilment establishes biomass as world's fourth largest energy source after oil, coal and gas. Pyrolysis, gasification and combustion are the prime technologies for thermal conversion of biomass. Gasification is the process where, through thermal decomposition in a low oxygen environment at temperatures of 800–900 °C, organic matter is converted to combustible gases with tars and chars as possible side-products. Air gasification results in the inferior quality gas (4–7 MJ/Nm^3 LHV). Oxygen as a gasification agent produces superior quality gas (10–16 MJ/Nm^3 LHV) but requires additional costs for oxygen production. A similar high quality gas can be produced by using a dual fluidized bed (DFB) system with steam as a gasification agent [1]. The fundamental idea of the DFB concept is to divide the gasifier into two fluidized bed reactors, a gasification reactor and a combustion reactor. The energy needed for the endothermic gasification reactions in the gasification reactor is provided by combustion of residual biomass called char in a combustion reactor. The energy released during combustion is transported to the gasification reactor along with the circulating bed material, thus making DFB gasifier a self sustained process.

The DFB gasifier can be regarded as a circulating fluidized bed (CFB) system with the bubbling bed gasifier in the return loop of the solids. A number of different CFB models have been developed and reviewed [2,3] but most of them are developed for coal combustion, i.e., for combustion of low volatile fuels. So far, biomass processing in CFBs has received little attention [4] and only a few attempts have been made to model biomass char as partial volatile fuel in CFB covering hydrodynamics and reaction kinetics. Further, confidentiality, numerous assumptions

* Corresponding author. Tel.: +43 1 58801x15965; fax: +43 1 58801 15999.
E-mail address: pkaushal@mail.zserv.tuwien.ac.at (P. Kaushal).

0016-2361/$ - see front matter © 2007 Published by Elsevier Ltd.
doi:10.1016/j.fuel.2007.03.032

Nomenclature

A	area (cross-sectional area) (m^2)
a	decay constant (m^{-1})
C_p	heat capacity (J/mol K)
D	diameter of column (m)
D	molecular diffusivity (m^2/s)
D_a	diameter of annulus (m)
D_c	diameter of core (m)
d_B	bubble diameter (equivalent diameter of a sphere) (m)
d_p	particle diameter (m)
d_{char}	char diameter (m)
g	gravity (m/s^2)
$\dot{H}$	enthalpy flow (J/s)
$H(T)$	enthalpy at temperature T (J/mol)
$\Delta H^0_{f,298}$	enthalpy of formation at 298.15 K (J/mol)
h_m	mass-transfer coefficient (kg/m^2 s bar)
$K_{B,E}$	mass-transfer coefficient between bubble and emulsion (s^{-1})
$K_{i\infty}$	elutriation rate constant (kg/m^2 s)
$k_{B,E}$	mass-transfer coefficient between bubble and emulsion (m/s)
k	reaction rate constant (dependent)
M_c	molecular weight of carbon (kg/mol)
$\dot{m}$	mass flow rate (kg/s)
m_{bed}	mass hold-up (bed material) (kg)
m_{char}	mass hold-up (char) (kg)
N	no of cells (–)
N_{or}	number of orifices (–)
$\dot{n}$	molar flow rate (mol/s)
n	order of reaction (–)
P	partial pressure (bar)
Q_B	volumetric flow rate in bubble (m^3/s)
Q_{EX}	gas exchange (m^3/s)
q	specific combustion rate of carbon on external surface (kg_{carbon}/m^2s)
R	universal gas constant (J/mol K)
$S_{B,E}$	surface area of bubble in contact with emulsion (m^2)
S_{char}	surface area of char (m^2)
Sh	Sherwood number (–)
T	temperature (K)
U_0	superficial velocity (m/s)
U_B	bubble velocity (m/s)
$U_{B\infty}$	velocity of a single isolated bubble (m/s)
U_E	velocity of gas in emulsion (m/s)
U_{mf}	minimum fluidization velocity (m/s)
U_t	terminal velocity (m/s)
Y	correction factor for modified two phase theory (–)
y	mole fraction (–)
z	height (m)
z_0	height of dense zone (m)

Greek symbols

δ_B	bubble fraction (–)
ε_{mf}	porosity at minimum fluidization condition (–)
ε_z	average porosity at height z (–)
ε_0	average porosity in dense zone (–)
ε_∞	Porosity above TDH (–)
ϕ	mechanism factor for primary surface product (1 for CO_2, 2 for CO) (–)
λ	air ratio (–)
μ	viscosity (Pa s)
ρ_p	density of particle (kg/m^3)

varied in a wide range makes the evaluation and comparison of these models very difficult. Hence, a mathematical model is developed for the riser to gain the better understanding of the process. The model is based on known approaches and with respect to the data available (for validation) from the DFB gasification plant at Guessing/Austria.

2. Model development

The present work focuses on the mathematical modelling of the combustion reactor indicated by the broken line in Fig. 1. The boundaries of the investigated system are the connecting chute at the bottom of the riser where bed material enters together with the residual biomass char from the gasification reactor and the cyclone at the top of the riser where the hot solids are separated from the flue gas stream. The objective of this study is to develop a model to predict the gas phase concentration and temperature profile along the height of the reactor.

The combustion reactor is divided into two zones namely dense and transport zone, having different hydrodynamic characteristics. Transport zone is further subdivided into middle and upper zone as shown in Fig. 1. Preheated air is introduced into the riser at three different points which are termed as bottom air, primary air and secondary air. Preheated gaseous fuel (i.e., recycled producer gas from the gasifier) is also introduced into the reactor to control the temperature of the entire system.

Each zone is further divided into cells and within each cell the local hydrodynamic, kinetic and thermodynamic variables are evaluated. Cells are solved sequentially with output of the Nth cell considered as input for the $(N+1)$th cell. The energy conservation equation is solved across the entire zone, and it is assumed that within a zone the temperature is uniform. This assumption is based on, efficient solids mixing and the dominance of the solid's heat capacity within a fluidized bed. The inputs for the model are the riser geometry, particle properties, gas composition and flow rate (Table 1)

Please cite this article in press as: Kaushal P et al., Model development and validation: Co-combustion of residual ..., Fuel (2007), doi:10.1016/j.fuel.2007.03.032

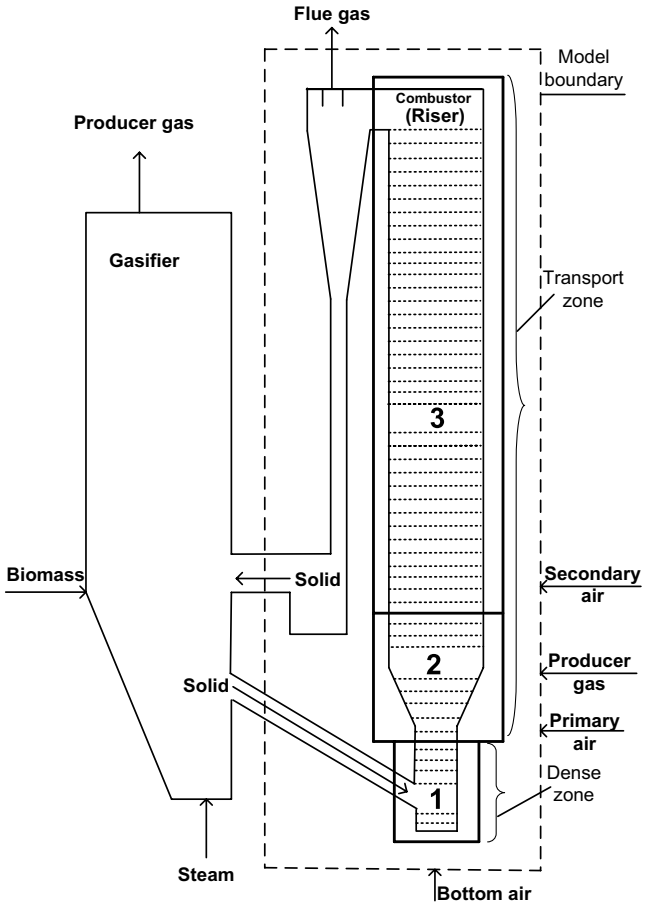

Fig. 1. Model structure and boundaries (1: dense zone, 2: middle zone, 3: upper zone).

Model assumptions:

The system is one-dimensional and in steady state.
Gases are ideal and in plug flow.
Solids are uniform in size and well mixed.
Each of the three main zones has a uniform temperature.
The mass transfer of a single gas species between the emulsion phase and bubble phase is modelled by a mass-transfer coefficient (k_{BE}).

Table 1
Input parameters to the model (typical operating condition from Guessing plant)

Diameter of column	0.61	(m)
Height of column	12	(m)
Diameter of particle	500E−6	(m)
Diameter of coke	0.001	(m)
Density of bed material	2960	(kg/m^3)
Density of coke	600	(kg/m^3)
Bed circulation	37	(kg/s)
Temperature of gasifier	883	(C)
Bottom air feed rate	700	(Nm^3/hr)
Primary air feed rate	2222	(Nm^3/hr)
Secondary air feed rate	1043	(Nm^3/hr)
Char composition (C, H, O)	(0.82, 0.04, 0.14)	(wt/wt)

The hydrodynamic parameters are evaluated based on the properties of bed which is classified as Geldart group B.

The flow regime map of Grace [5] between dimensionless velocity (U^*) and dimensionless particle diameter (d_p^*) confirmed that the fluidization state of the dense bed is in bubbling mode. Gas balance based on superficial velocity is

$$U_0 = U_B\delta_B + (1-\delta_B)\varepsilon_{mf}U_E. \quad (1)$$

Two phase theory (TPT) assumes that visible bubble flow corresponds to the excess gas velocity i.e., $(U_0 - U_{mf})$. However, this theory tends to overestimate the bubble flow. In order to limit the deviation from observations, the modified two phase theory [6] is used, where

$$Q_B = Y(U_0 - U_{mf}). \quad (2)$$

Y is always below unity and usually in the range from 0.7 to 0.8. Y can also be 0.3 for coarse particles. The reported values of Y in literature scatter in a wide range [7]. Y is a function of the height above the gas distributor and hence the correlation proposed by Johnsson et al. [8] is used to estimate the value of Y.

$$Y = \frac{0.26 + 0.7\exp(-0.0033d_p)}{[0.15 + (U_0 - U_{mf})]^{0.33}}\left(z + 4\sqrt{\frac{A}{N_{or}}}\right)^{0.4}. \quad (3)$$

Bubbles are formed as soon as the superficial gas velocity exceeds minimum fluidization velocity. The bubble size is one of the most critical parameters when modelling fluidized beds, it affects the bubble rising velocity, the bubble fraction and the mass transfer between bubble and emulsion phase. As the bed height increases, bubbles coalesce and the bubble size increases. The bubble size is calculated as a function of bed height and it is assumed that all bubbles at any cross section are of uniform size [9].

$$d_B = 0.54(U_0 - U_{mf})^{0.4}\left(z + 4\sqrt{\frac{A}{N_{or}}}\right)^{0.8} g^{-0.2}. \quad (4)$$

Bubble's interaction influences the bubble rising velocity and the common adaptation for bubble rising velocity given by Davidson and Harrison [10] is used in this work

$$U_B = U_{B,\infty} + (U_0 - U_{mf}). \quad (5)$$

For bubbles, the rising velocity of a single isolated bubble is given below.

$$U_{B,\infty} = 0.71\sqrt{gd_B} \quad (6)$$

There is no theoretical basis to support this correlation, however, numerical simulations [11,12] show that this approximation is reasonable.

It is evident that a major part of the gas flows in the bubble phase. Thus, the interphase mass transfer between bubble and emulsion phase is essential for the gas–solid reactions. The interphase mass transfer is modelled by a semi-empirical approach using a mass-transfer coefficient, the exchange area and the concentration gradient according to Sit and Grace [13]

$$K_{BE} = \frac{U_{mf}}{4} + \sqrt{\frac{4\varepsilon_{mf} D U_B}{\pi d_B}}. \quad (7)$$

Fig. 2 shows the gas flow streams in the dense zone and the gas exchange between the bubble and emulsion phase. After the injection of primary air into the combustion reactor, the superficial gas velocity is increased and the reactor operates in fast fluidization regime. Fast fluidized beds exhibit strong radial gradients with respect to solid hold-up and solid movement. Near the column walls the particle moves downwards and the concentration of particles is higher than in the core of the reactor, where particles are transported upwards. Different approaches are proposed to describe fast fluidized bed reactors [14–16]. In the present work, the transport zone is modelled by a simplified core-annulus approach. The axial mean voidage is calculated using an exponential decay function as proposed by Zenz and Weil [17]

$$\frac{\varepsilon_z - \varepsilon_\infty}{\varepsilon_0 - \varepsilon_\infty} = \exp[-a(z - z_0)]. \quad (8)$$

Unknown parameters in Eq. (8) are the decay factor 'a' and the porosity above transport disengaging height 'ε_∞'. The value of 'a' varies widely in the literature and is approximately in the range of 2–6.4 m^{-1} [18]. Cold flow studies of the process showed that the decay constant depends on the fluidizing velocity to a higher power than one. Thus, the correlation proposed by Adanez et al. [19] was adopted.

$$a(U_0 - U_t)^2 D^{0.6} = K. \quad (9)$$

Based on the pressure drop measurement at standard conditions the constant K was determined to be $K = 8.6$. The value of ε_∞ is determined from the particle elutriation rate constant $K_{i\infty}$ for a mono-sized bed material:

$$1 - \varepsilon_\infty = \frac{K_{i\infty}}{\rho_p (U_0 - U_t)} \quad (10)$$

$$K_{i\infty} = 0.011 \rho_p \left(1 - \frac{U_t}{U_0}\right)^2. \quad (11)$$

The voidage in the core at a given height is calculated from the mean porosity ε_z at that height [20]

$$\varepsilon_C = 1 - 0.6(1 - \varepsilon_z). \quad (12)$$

It is assumed that the annulus is maintained at minimum fluidization conditions. The diameter of the core increases with the height of the riser and is estimated from Eq. (13).

$$\varepsilon_a D_a^2 + \varepsilon_c D_c^2 = \varepsilon_z D^2. \quad (13)$$

Unlike dense zone in the transport zone it is assumed that, there is a single gas stream across both the core and annulus. The local variables (e.g., reaction rate, hold-ups, etc.) are calculated separately for core and annulus but the mass balances are applied across the whole cell as shown by the broken line in Fig. 3.

Char combustion is in general a complex process due to the combination of different mechanisms as mass transfer, chemical reaction and heat transfer. In general, combustion of char begins after the evolution of volatiles. Sometimes, especially for large particles, there is a significant overlapping of these processes. The char composition is an important model parameter and is assumed to be a homogeneous matrix of carbon, hydrogen and oxygen. Carbon present in char is modelled as non-volatile fuel subject to heterogeneous oxidation with O_2 and if no O_2 is present then with H_2O. The primary products in the case of char combustion are CO and CO_2 represented by reaction A.

$$(1+\beta)C + (1 + \frac{\beta}{2})O_2 \rightarrow \beta CO + CO_2, \quad (A)$$

where β is a stoichiometric coefficient for char combustion describing the ratio of CO to CO_2 and is a function of surface temperature [21]. Char gasification reaction (B) is also considered in the model.

$$C + H_2O \xrightarrow{k} CO + H_2. \quad (B)$$

The carbon combustion model is based on the combined effects of gas film diffusion and reaction kinetics on a shrinking particle and it is assumed that the diameter of the char particle decreases while the density of the char remains constant. Oxidation occurs in a thin layer close to the particle surface and no ash layer is formed. The combustion rate in term of mass transfer through the gas film can be described as

$$q = h_m (P_{O_2,g} - P_{O_2,s}) \quad (14)$$

$$h_m = \frac{M_c \phi Sh D}{d_{char} RT}. \quad (15)$$

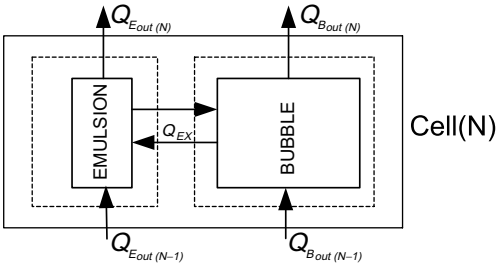

Fig. 2. Gas balances in dense zone.

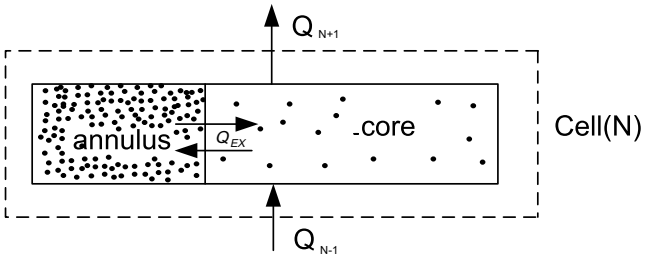

Fig. 3. Gas balances in transport zone.

The chemical reaction rate of carbon with oxygen per unit time and per unit external surface area of the particle is

$$q = kP^{n}_{O_{2,S}} S_{\text{char}}. \quad (16)$$

Eqs. (14) and (16) are solved under steady state assumption,. The data obtained from experiments allow minimization of the root of mean square for the Arrhenius expression [22].

The hydrogen and oxygen present in char are modelled as volatile fuel. Hydrogen and oxygen are released in a way that the char composition remains constant as conversion proceeds. The hydrogen and oxygen released react to form water (C). The ratio of CO, CO_2, H_2, O_2 and H_2O release is calculated from the combustion kinetics of carbon and balances of char.

$$H_2 + \frac{1}{2}O_2 \Longleftrightarrow H_2O. \quad (C)$$

Carbon monoxide released from char is modelled to undergo combustion reaction and shift reaction

$$CO + \frac{1}{2}O_2 \Longleftrightarrow CO_2 \quad (D)$$

$$CO + H_2O \Longleftrightarrow CO_2 + H_2. \quad (E)$$

The effect of the CO shift reaction becomes pronounced when oxygen within a zone is consumed. As shown in Fig. 1, a small amount of producer gas is also recycled into the middle zone of the combustion reactor. The combustion kinetics and composition of the producer gas are given in Tables 2 and 3, respectively.

The elementary mass balances inside every single cell is covered by the stoichiometry of the homogeneous and heterogeneous reaction formulations. The mass balance for solid carbon and the energy balance are applied globally across each of the three zones as indicated in Fig. 1.

Char is evenly distributed in each cell of dense zone as

$$m_{c_K} = \frac{1}{N}(m_c), \quad (17)$$

where as in transport zone char is distributed in cells in such a way that the ratio of bed hold-up in adjacent cell is the same as the ratio of char hold-up.

$$\frac{m_{\text{bed}_{k+1}}}{m_{\text{bed}_k}} = \frac{m_{\text{char}_{k+1}}}{m_{\text{char}_k}}. \quad (18)$$

Globally across the entire zone, the char balance is formulated as

$$\dot{m}_{\text{Char,out}} + \dot{m}_{\text{Char,reacted}} = \dot{m}_{\text{Char,in}}. \quad (19)$$

The general carbon balance of each zone is written as

$$\dot{m}_{c_{\text{in}}} = \dot{m}_{c_{\text{out}}} + \sum_{k=1}^{N} \frac{\mathrm{d}m_c}{\mathrm{d}t}. \quad (20)$$

All feed rates are input parameters to the model. Because of the assumption of uniform char concentration in the solids, the char exit rate and the char hold-up in the zone are directly linked to each other. The char conversion rate from solid to gas is dependent on several parameters within each cell and depends directly on the available char surface area within the zone, the zone temperature and partial pressures of the reactants, i.e., O_2 or H_2O.

The energy balance is formulated globally across the entire zone using total enthalpies including the standard enthalpy of formation with the assumption that the total amount of energy entering the system is actually leaving the system.

$$\sum \dot{H}_{\text{out}} = \sum \dot{H}_{\text{in}} \quad (21)$$

$$H(T) = \Delta H^{0}_{\text{f},298} + \int_{T=298.15}^{T} C_p(T)\,\mathrm{d}T. \quad (22)$$

The enthalpy of ideal gas mixtures is calculated using the NASA polynomials with coefficients reported by Burcat and McBride [29]. The enthalpy of the inert bed material is calculated by interpolation of data reported by Barin [30]. The sensible heat of char is calculated using the correlations reported by Merrick [31]. The enthalpy of forma-

Table 2
Reaction rates

	Reactions	Reaction rate	K	Ref.
A	$(1+\beta)C + (1+\beta/2)O_2 \rightarrow CO + CO_2$	$q = K[P_{O2}]^{0.5}$ Schar	$8.56\times10^{-2}\exp(-2237/T)$	[22]
B	$C + H_2O \rightarrow CO + H_2$	$q = K[P_{H2O}]^{0.57}$	$2.62\times10^{8}\exp(-237000/T)$	[23]
C	$H_2 + 1/2\ O_2 \rightarrow H_2O$	$r_{H2} = K[H_2]^{1.5}[O_2]$	$1.63\times10^{9}\ T^{3/2}\exp(-3420/T)$	[24]
D	$CO + 1/2\ O_2 \rightarrow CO_2$	$r_{CO} = K[CO][O_2]^{0.5}[H_2O]^{0.5}$	$3.25\times10^{7}\exp(-15098/T)$	[25]
E	$CO + H_2O \rightarrow H_2 + CO_2$	$r_{CO} = K[CO][H_2O]$	$0.03\ \varepsilon\exp(-7249/T)$	[26]
F	$CH_4 + 3/2\ O_2 \rightarrow CO + 2H_2O$	$r_{CH4} = K[CH_4]^{0.7}[O_2]^{0.8}$	$4.68\times10^{18}\ T^{0.5}\exp(-20087/T)$	[27]
G	$C_2H_4 + 2O_2 \rightarrow 2CO + 2H_2O$	$r_{C2H4} = K[C_2H_4][O_2]$	$1.0\times10^{12}\exp(-20844/T)$	[28]
H	$C_2H_6 + 5/2\ O_2 \rightarrow 2CO + 3H_2O$	$r_{C2H6} = K[C_2H_6][O_2]$	$2.34\times10^{18}\ T^{0.5}\exp(-20087/T)$	[27]
I	$C_3H_8 \rightarrow C_2H_4 + CH_4$	$r_{C3H8} = K[C_3H_8]$	$1.0\times10^{12}\exp(-21145/T)$	[28]

Table 3
Producer gas composition

LHV (dry)	Composition (vol%)								
(MJ/Nm^3)	CO	CO_2	CH_4	C_2H_4	C_3H_8	H_2	H_2O	O_2	N_2
13.1	21	20	10	2	1	35	9	0	2

Please cite this article in press as: Kaushal P et al., Model development and validation: Co-combustion of residual ..., Fuel (2007), doi:10.1016/j.fuel.2007.03.032

tion for char is calculated from the heating value, estimated from ultimate analysis using the Boie formula [32]. $\dot{H}_{out}$ is a function of the exit temperature of the respective streams. Since a uniform temperature is assumed inside the zone, the problem is reduced to the determination of the two variables char hold-up and temperature in order to fulfil Eqs. (19) and (21).

A two-dimensional Newton–Raphson algorithm is applied where the components of the Jacobian matrix are calculated analytically. The iteration is performed for each of the three zones where the order is again from bottom towards top of the combustion reactor. After convergence, the model yields the gas phase concentration profiles, the temperature in each zone, the solid char flow rate leaving the reactor and the apparent global air ratio λ which is defined by neglecting the bypassing fraction of the char (i.e., only the actually converted char is considered).

$$\lambda = \frac{[\dot{n}y_{O_2}]_{in}}{[\dot{n}y_{O_2}]_{in} - \left[\dot{n}\{y_{O_2} - 0.5y_{CO} - \sum_{C_xH_y}(x+0.5y)y_{C_xH_y}\}\right]_{out}}. \quad (23)$$

3. Results and discussion

The solution of the mathematical model represents simultaneous convergence of the conservation equation (for which different subroutines have been defined). Table 1 lists the input parameters for a typical operation case. The average residence time of the gas in the combustion reactor is in the range of 1.0–1.5 s while the air ratio in the standard condition is approximately 1.02.

3.1. Predicted profile of gas composition

Fig. 4a shows the concentration profile inside the bottom bed (dense zone) separately for the bubble and emulsion phases. As can be seen, the concentration of oxygen in emulsion phase goes down swiftly and when O_2 is completely consumed, the char gasification and shift reaction dominates; this can be observed by the increased concentration of H_2 and CO_2 in emulsion phase at the relevant heights. In the bubble phase, the concentrations of CO and H_2 are very low while that of oxygen is relatively high. This is one of the major limitations of one-dimensional model that it fails to explain the three-dimensional mixing effect. Nevertheless such behaviour of dense bed is often reported [4,33]. The overall gas composition profiles along the riser height are shown in Fig. 4b. The concentration profiles of CO, CO_2, H_2 and H_2O locally go down at the height of 2 and 4 m due to dilution effect caused by primary and secondary air addition. Results show that the producer gas added in the middle zone (rich in combustible gas) quickly combusts to CO_2 and H_2O. The predicted gas-profile inside the riser could not be verified at the demonstration plant at Guessing because of the lack of measurents. Therefore, to validate the model, the operating parameters of the present model were adjusted in order to match with the operating parameters of the fluidized bed boiler at Chalmers University (Sweden), reported by Adanez et al. [4]. Newton–Raphson method was used to iterate the wood feed rate to fit the excess air ratio reported by Adanez et al. Fig. 5 shows a comparison between the measured and predicted oxygen concentrations along the height of riser. The oxygen profile predicted by the present model is in fair agreement with the measured values [4,34]. As seen in Fig. 5, an increase in oxygen concentration with height is not realistic and as indicated by Amand et al. [33], it can be attributed to an insufficient penetration depth and mixing of the secondary air flow. Nevertheless Adanez et al. investigated various possibilities to deal the mixing problem in one-dimensional model.

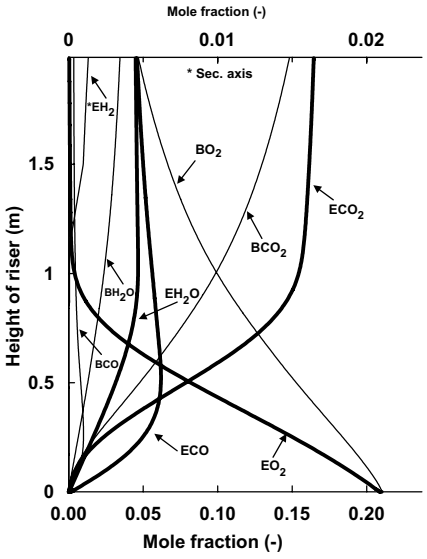

Fig. 4a. Gas composition profile in dense bed. B: bubble; E: emulsion.

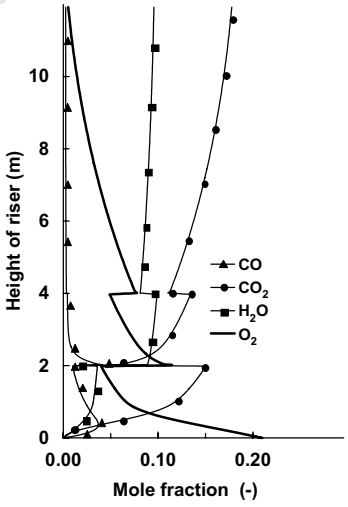

Fig. 4b. Average gas composition profile along height of riser.

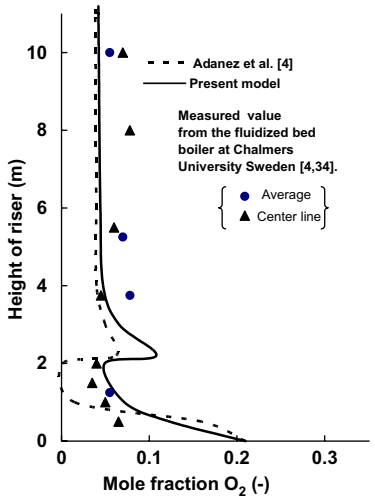

Fig. 5. Comparison of model prediction for O_2 concentration.

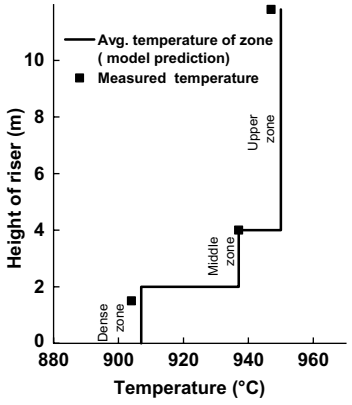

Fig. 6. Measured and predicted temperature.

3.2. Predicted temperature profile

At the demonstration plant at Guessing, the temperature inside the riser is measured at three different heights. The predicted temperature profile is in good agreement with the measured value (Fig. 6). A little over-prediction in temperature is observed but the deviation in temperature prediction is less than 5 K.

3.3. Effect of char diameter

Fig. 7 shows the effect of char feed rate on air ratio at different char sizes. It should be noted that all the other operating parameter were fixed except char feed rate and size. Each curve in Fig. 7 were generated by changing the char feed rate at a given constant char size. Result shows that with increase in char feed rate, the air ratio decreases. The slope of the curve changes at an air ratio of 1, suggesting that for lower char feed rates, char size have a very prominent effect on char conversion. Simulation shows that for constant char feed of 0.8 kg/s air ratio changes from 0.85 to 0.93 when char size is changed from 4 to 8 mm. Therefore, it can be concluded that smaller size favours char conversion. The simulation results also show that the residual char from the gasifier is only partly converted in the riser and the remaining un-combusted char is circulated back into the gasification reactor and potentially leads to an increase of char hold up in the dual fluidized bed system. Fig. 8 shows the exit CO concentration for the various points shown in Fig. 7. It can be seen in the figure, that for air ratio below 1, the CO concentration increases abruptly. It also shows that irrespective of the char size the CO concentration follows the same trend line suggesting that exit CO concentration is a strong function of air ratio and is independent of char size.

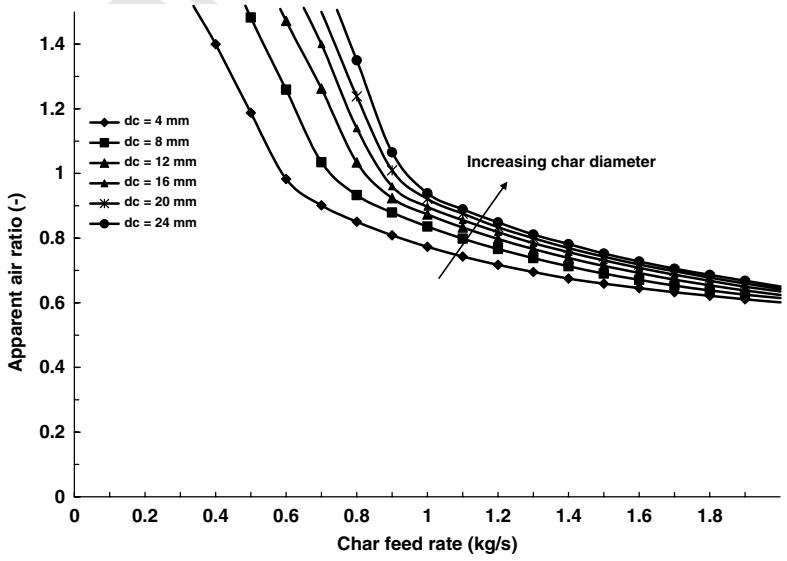

Fig. 7. Effect of char feed rate on apparent air ratio.

Please cite this article in press as: Kaushal P et al., Model development and validation: Co-combustion of residual ..., Fuel (2007), doi:10.1016/j.fuel.2007.03.032

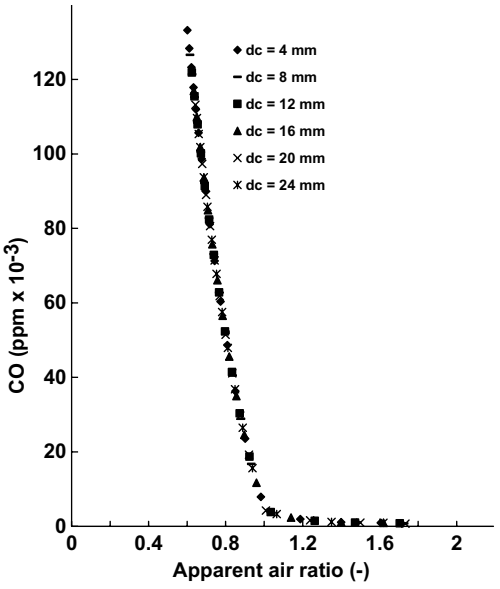

Fig. 8. CO concentration in flue gas.

4. Conclusions

A one-dimensional steady state model of a riser has been developed to analyze the combustion of biomass char in circulating fluidized bed. The model is based on mass and energy balances. The model includes different sub-models that are linked together to describe the overall combustion process. The hydrodynamic sub-model highlights the physical characteristics of the bed material while the reaction sub-model deals with the chemical reactions in the different zones of the combustion chamber (riser). The model is fuel flexible and offers the opportunity to evaluate different fuel types over wide range of composition both for solid and gases. Global reaction rates are used for the description of chemical kinetics. Model validations have been performed with measured results obtained at both 8 MWth dual fluidized bed gasification plant at Guessing, Austria and with literature data on the 12 MWth circulating fluidized bed boiler at Chalmers University (Sweden). The predicted trends are qualitatively compared with the published data [4,33] and it turns out that they are in fair agreement. The model predictions show that the gas composition varies significantly in the upper section above the secondary air injection. Simulation results also show that smaller size of wood or char favours the overall performance of the gasifier.

Acknowledgement

The authors gratefully acknowledge the financial support from RENET Austria (K_{net}/K_{ind} public fund program, Austria).

References

[1] Hofbauer H. CFB – steam gasification. 14th European biomass conference and exhibition biomass for energy, industry and climate protection. 17–21 October 2005, Paris, France.
[2] Grace JR, Avidan AA, Knowlton TM. Circulating fluidized beds. New York: Chapman and Hall; 1997.
[3] Basu P. Combustion of coal in circulating fluidized-bed boilers: a review. Chem Eng Sci 1999;54(22):5547–57.
[4] Adanez J, Gayan P, de Diego LF, Garcia-Labiano F, Abad A. Combustion of Wood Chips in a CFBC. Modeling and Validation. Ind Eng Chem Res 2003;42(5):987–99.
[5] Grace JR. Fluidized beds as chemical reactors. In: Geldart D, editor. Gas Fluidization Technology. New York: John Wiley and Sons; 1986.
[6] Grace JR, Clift R. The two phase theory of fluidization. Chem Eng Sci 1974;29(2):327–34.
[7] Baeyens J. Gas fluidization, short course. University of Bradford: Institute of Chemical Engineering; 1981.
[8] Johnsson F, Andersson S, Leckner B. Expansion of a freely bubbling fluidized bed. Powder Technol 1991;68(2):117–23.
[9] Darton RC, La Nauze RD, Davidson JF, Harrison D. Bubble growth due to coalescence in fluidized beds. Trans Inst Chem Eng 1977;55(4):274–80.
[10] Rowe PN. Experimental properties of bubbles. In: Davidson JF, Harrison D, editors. Fluidization. London: Academic Press; 1971. p. 21–189.
[11] Davidson JF, Harrison D. Behaviour of a continuously bubbling fluidized bed. Chem Eng Sci 1966;21(9):731–8.
[12] Grace JR, Harrison D. Behaviour of freely bubbling bed. Chem Eng Sci 1969;24(3):497–508.
[13] Sit SP, Grace JR. Interphase mass transfer in an aggregative fluidized bed. Chem Eng Sci 1978;33(8):1115–22.
[14] Fane AG, Wen CY. Fluidized-bed reactors. In: Hetsroni G, editor. Handbook of multiphase systems. Washington: Hemisphere; 1982. p. 8-105–51.
[15] Grace JR. Modeling and simulation of two-phase fluidized bed reactors. In: Lasa Hde. Editor. Chemical reactor design and technology, Martinus Nijhoff; 1986, p. 245–89.
[16] Van Swaaij WPM. The design of gas–solids fluid bed and related reactors. In: Luss D, Weekman VW, editors. ACS Symp Ser 72. New York: American Chemical Society; 1978. p. 193–222.
[17] Zenz FA, Weil NA. A theoretical-empirical approach to the mechanism of particle entrainment from fluidized beds. AIChE J 1958;4(4):472–9.
[18] Löffler G, Kaiser S, Bosch K, Hofbauer H. Hydrodynamics of a dual fluidized-bed gasifier – part I: simulation of a riser with gas injection and diffuser. Chem Eng Sci 2003;58(18):4197–213.
[19] Adanez J, Gayan P, Garcia-Labiano F, de Diego LF. Axial voidage profiles in fast fluidized beds. Powder Technol 1994;81(3):259–68.
[20] Namkung W, Kim SD. Gas back mixing in a circulating fluidized bed. Powder Technol 1998;99(1):70–8.
[21] Arthur JA. Reaction between carbon and oxygen. Trans Faraday Soc 1951;47:164–78.
[22] Winter F, Wartha C, Hofbauer H. Characterization and emission of single fuel particles under FBC condition. Third international conference on combustion technologies for a clean environment, 3–6 July 1995, Lisbon, Portugal.
[23] Barrio M, Gobel B, Risnes H, Henriksen U, Hustad JE, Sorensen LH. Steam gasification of wood and the effect of hydrogen inhibitation on the chemical kinetics. Progress in thermochemical biomass conversion, September 2000, Tirol, Austria.
[24] Vilienskii TV, Hezmalian DM. Dynamics of the combustion of pulverized fuel. energiya 1978, Moscow.

[25] Dryer FL, Glassman I. High-temperature oxidation of CO and CH_4. Fourteenth international symposium on combustion, The Combustion Institute: Pittsburgh, PA, 1973, p. 987–1003.
[26] Weimer A, Clough D. Modeling a low pressure steam oxygen fluidized bed coal gasifying reactor. Chem Eng Sci 1981;36(3):548–67.
[27] Zimont VL, Trushin YM. Total combustion kinetics of hydrocarbon fuels. Combust, Explosion Shockwaves 1969;5(4):567–73.
[28] Van der Vaart DR. PhD Thesis, University of Cambridge, 1985, England.
[29] Burcat A, McBride B. Ideal gas thermodynamic data for combustion and air pollution use. Technion isreal Institute of Technology, Aerospace Engineering Report, 1997, TAE 804 (Garfield.chem.elte.hu/Burcat/burcat.html).
[30] Barin I. Thermochemical data of pure substance. 2nd ed. Germany: VCH; 1993.
[31] Merrick D. Mathematical models of the thermal decomposition of coal part 1–6. Fuel 1983;62(5):534–70.
[32] Boie W. Vom Brennstoff zum Rauchgas – Feuerungstechnisches Rechnen mit Brennstoffkenngrößen und seine Vereinfachung mit Mitteln der Statistik, Teubner, Leipzig, 1957.
[33] Yan HM, Craig H, Zhang D. Mathematical modelling of a bubbling fluidized bed coal gasifier and the significance of net flow. Fuel 1998;77(9/10):1067–79.
[34] Amand L, Lyngfelt A, Karlsson, M, Leckner B. Fuel loading of a fluidized bed combustor burning bituminous coal, peat or wood chips. Report A97-221 1999; Deparment of Energy Conversion, Chalmers University of Technology: Goeteborg, Sweden. (<http://www.entek.chalmers. se/~leam/Input_model/Fuel_loading1/Charload_rev1.pdf>).